UDC 622.235.5
DOI: https://doi.org/1034169/2414-0651.2025.1(45).56-64

Yu. I. VOITENKO, *Doctor of Technical Sciences Professor*

V. A. VOSKOBOINICK, *Doctor of Technical Sciences Associate Professor*
https://orcid.org/0000-0003-2161-6923

V. V. BOYKO, *Doctor of Technical Sciences, Professor (Institute of Hydromechanics of the NAS of Ukraine, Kyiv)*

I. B. CHEPKOV, *Corresponding Member of the National Academy of Sciences of Ukraine Doctor of Technical Sciences, Professor*
https://orcid.org/0000-0002-4294-4152

E. O. OSTAPCHUK
https://orcid.org/0000-0002-8095-0203 (Central Scientific Research Institute of Armament and Military Equipment of Armed Forces of Ukraine, Kyiv)

O. F. NEMCHYN, *Doctor of Technical Sciences Professor*
https://orcid.org/0000-0001-9160-2768

D. V. YEVDOSHCHUK
(Institute of Engineering Thermophysics of the NAS of Ukraine, Kyiv)

EVALUATION OF AIR SHOCK WAVE PARAMETERS AND PROTECTION AGAINST THEM WITH BALLISTIC FOAM CONCRETE

The parameters of the air shock wave during the detonation of a standard charge of TNT with a mass of 1 kg when it falls on barriers made of ballistic foam concrete of four types and the air shock wave flow around this barrier were studied. The thickness of the ballistic foam concrete samples is 300 mm, the density is 600 kg/m³. Empirical formulas of M.A. Sadovsky were used for the calculations. A satisfactory match of the experimental data with the parameters calculated according to the formulas of M.A. Sadovsky was established. In the experiments, it was shown that the amplitude of air shock wave behind the barrier made of ballistic foam concrete decreases by an average of 8–30 times. Approximate estimates based on the research data of other authors (Belinsky I.V., Khristoforov B.D.) predict a reduction of the compression wave that propagates through ballistic foam concrete by no more than 5–10 times. As a result of experimental researches, it was found that the shock waves from the explosions turned the relatively insignificant upper layer of the foam concrete slabs, which is the «sacrificial» layer, into a compressed powder due to the destruction of the interpore partitions. In the plane of the surface of the foam concrete slabs, the «sacrificial» layer was described by an imaginary circle, which is the projection of the explosion. The size of the «sacrificial» layer of ballistic foam concrete destroyed by air shock wave from the frontal side does not exceed 20–40 mm. Spalling phenomena from the back side of the ballistic foam concrete samples were not observed when the air shock wave fell with amplitude of 0.4–0.6 MPa. There are 2 types of ballistic foam concrete with the most effective damping of the compression wave in it. It was established that the most effective in terms of protecting critical infrastructure facilities from the action of air shock waves are foam concrete models of protective structures, which are reinforced with fiber of composition «A» and «B» with a reinforcing layer of composite material applied. It was determined that in these models the deepest zones of destruction of ballistic foam concrete were observed on the front side of the protective structure.

Keywords: *charge, air shock wave, protective structures, ballistic foam concrete, critical infrastructure, «sacrificial» layer.*

INTRODUCTION

The task of assessing the main parameters of air shock waves: excess pressure at the air shock waves front, impulse and duration of action in the compression phase has always been relevant in the design of explosive works [1–4]. It acquires particular importance in wartime conditions for assessing the impact of various means of destruction on the environment. In addition, increasing the accuracy and reliability of such assessments allows designing effective structures for protecting important infrastructure facilities and new materials for their construction. The availability of data on the parameters of air shock waves, acoustic waves and seismic waves allows us to accurately determine the type of ammunition that hit a particular object in the event of a ground or surface explosion. The main means of destroying civilian objects outside the front-line areas are unmanned aerial vehicles with an explosive mass of ≈(20–40) kg TNT and cruise and ballistic missiles with an explosive mass in the warhead of ≈(200–400) kg.

The purpose of the article is to analyze empirical formulas for calculating the parameters of the air shock waves during air, ground and surface explosions of charges of different masses; experimental assessment of their reliability; assessment of dynamic strength, destruction of samples of new building materials – ballistic foam concrete under the action of air shock wave of low and medium intensity.

MATERIALS AND METHODS OF RESEARCH

The research was conducted at a military training ground on a specially created experimental stand. Fig. 1 shows a photograph of a model of a ballistic foam concrete protective structure and a diagram of the location of the experimental stand, test specimens, detonation points and measuring equipment.

The stand for installing the test specimens is a prefabricated reinforced concrete structure (Fig. 1a), which is constructed from two reinforced concrete slabs with dimensions in plan of 2000 x 2000 mm, 300 mm thick, made of concrete of class C16/20, installed vertically at an angle of 90º to each other, on four foundation blocks measuring

1000 x 1000 x 1200 mm, reinforced with a supporting metal frame.

The ballistic foam concrete protective structure samples consisted of the following elements:

– a slab of monolithic ballistic foam concrete, aged for 23 days;
– a slab of monolithic ballistic foam concrete, aged for 23 days with a reinforcing layer of composite material applied.

The number of samples and the parameters of monolithic ballistic foam concrete slabs were determined by the tasks set in the experimental tests. The following parameters were established:

sample No. 1: the ballistic foam concrete slab with a density of 600 kg/m^3, dimensions in plan 2000 x 1000 mm, thickness 300 mm;

sample No. 2: the ballistic foam concrete slab with a density of 600 kg/m^3, dimensions in plan 2000 x 1000 mm, thickness 300 mm, with a reinforcing layer of composite material applied;

sample No. 3: the ballistic foam concrete slab with a density of 600 kg/m^3, dimensions in plan 2000 x 1000 mm, thickness 300 mm, reinforced with fiber of composition «A», with a reinforcing layer of composite material applied;

sample No. 4: the ballistic foam concrete slab with a density of 600 kg/m^3, dimensions in plan 2000 x 1000 mm, thickness 300 mm, reinforced with fiber of composition «B», with an applied reinforcing layer of composite material.

In front of the ballistic foam concrete protective structure model, a wooden mast was installed at a distance of 1.4–1.5 m from the model, where a 1 kg TNT charge was fixed at a height of 1 m from the ground level (Fig. 2a). Each slab on the inside of the angle they form has two niches, which are located at a distance of 1000 mm from the lower edge of the slabs and at a distance of 500 mm from the side edges of the slabs, with a distance of 1000 mm between them. The niches are intended for installing dynamic pressure sensors and laying plastic tubes for passing cables leading to them (Fig. 2b).

The sensors were located near the front surface of the test specimens, as shown in Fig. 2a, as well as the front surface of the reinforced concrete slab or on the back side of the ballistic foam concrete slabs, as shown in Fig. 2b. During the tests, a separate charge was detonated in front of one pair of ballistic foam concrete (samples No. 1 and No. 2) and then in front of the other pair (samples No. 3 and No. 4).

During the tests, the following were measured: dynamic pressure (MPa, at) of air shock waves and dynamic parameters (frequency (kHz), acceleration (m/s²)) of

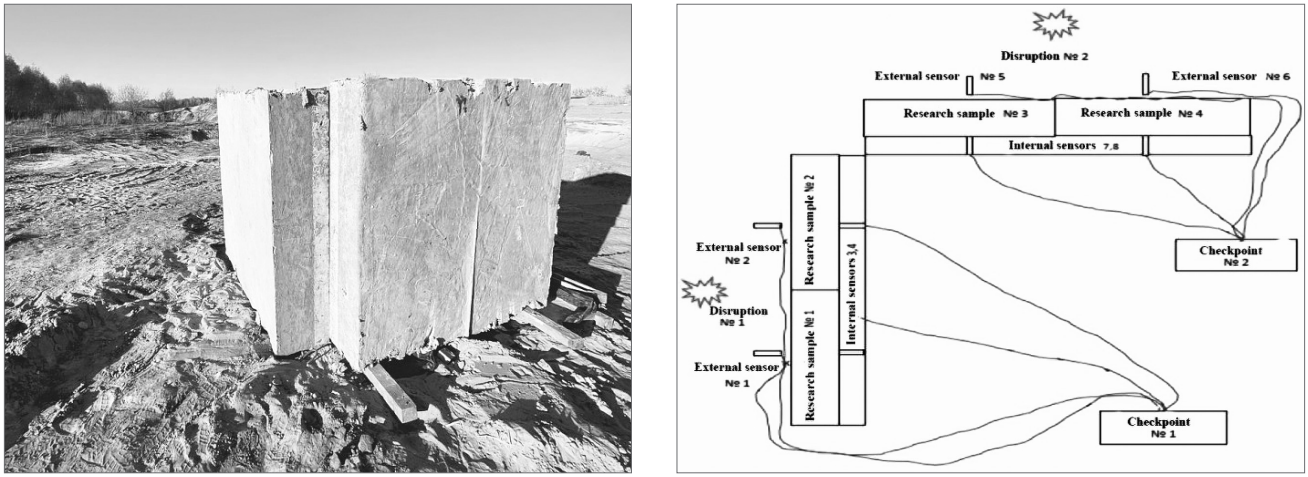

a) **b)**

F i g . 1. Model of a foam concrete protective structure (a) and layout of the elements of the experimental stand (b)

a) **b)**

F i g . 2. Model of the ballistic foam concrete protective structure element before the explosion: front view with the placement of the TNT charge and pressure sensors (a) and the location of the sensors on the back side of the concrete slab (b)

vibrations of reinforced concrete slab structures protected by experimental samples of ballistic foam concrete slabs [5–7], when exposed to an air shock wave caused by the detonation of an explosive; the thickness of the «sacrificial» layer of ballistic foam concrete slabs (mm) formed on their surface when damping shock waves.

The following measuring equipment was used to conduct the tests:

– pressure sensors of the PS2300V5 type from the company «Dytran Instruments, Inc.» (USA), which record the maximum pressure from the shock wave on the surface of the ballistic foam concrete slab and on the surface of the reinforced concrete slab (test stand) at the time of the explosion (Fig. 3);
– equipment for transmitting signals from the sensors to a computer and recording them;
– a scale ruler for measuring the thickness of the «sacrificial» layer of ballistic foam concrete slabs.

RESEARCH RESULTS AND DISCUSSION

According to the program and research methodology, methods of mathematical and physical simulation of the interaction of air shock waves with models of the ballistic foam concrete protective structures were applied. As a result, the results of calculations of the main parameters of the air shock waves, the excess pressures that it creates and the loads on the models of foam concrete structures were obtained, as well as the acoustic-dynamic characteristics of the air shock wave and their interaction with the surface of the ballistic foam concrete protective structure and the degree of reduction of the shock pressure on the structures protected by the ballistic foam concrete structure were measured [8–11].

Results of physical modeling (according to Sadovsky M.A.)

For the explosion of charges from a 50/50 TG mixture in air with normal initial conditions, the following formulas were obtained for calculating the main parameters of the air shock wave [12]:

$$\Delta P = 0.85\frac{C^{1/3}}{R} + 3.0\frac{C^{2/3}}{R^2} + 8.0\frac{C}{R^3},\ I = 20\frac{C^{2/3}}{R},$$
$$\tau_+ = 1.2C^{1/6}R^{1/2}, \qquad (1)$$

$$0.1 \le \frac{C^{1/3}}{R} \le 1.0,\ \left(0.1\frac{kg}{cm^2} \le \Delta P \le 10\frac{kg}{cm^2}\right), \qquad (2)$$

where ΔP is the excess pressure at the front of the incident shock wave; I is the pressure pulse; τ_+ – the duration of the pressure in the air shock wave in the compression phase.

The law of energy similarity in explosions consists in the fact that the charge as a source of a shock wave is characterized by energy E, which is proportional to the mass of the charge C ($E = CQ$, Q – heat of explosion of 1 kg of explosive). Taking into account chemical losses in explosions in relation to the specific heat of explosion allows us to recalculate the coefficients in these formulas for the case of any explosive. Since TNT was used in the experiments (Q_1=4185 kJ/kg, C_1=1 kg), and in the experiments [12] – TG 50/50 (Q_2=4856 kJ/kg), the condition of energy similarity will be the ratio $E_{TNT}=E_1=C_1Q_1=E_{TG}=E_2=C_2Q_2$. Whence C_2=0.862 kg. For C_1=40 kg $C_2\approx$34.5 kg; for C_1=400 kg $C_2\approx$344.7 kg.

Calculation according to formula (1) for the value of excess pressure on the air shock wave front for TNT charges weighing 1 kg, 40 kg, 400 kg (TG 50/50 – 0.862 kg, 34.5 kg and 344.7 kg) is given in Table 1. The notation in Table 1: ΔP – value of excess pressure on the air shock wave front; R_0 – radius of the charge; R – distance from the center of the charge in m for a charge weighing 1 kg of TNT (column No. 3), 40 kg (column 4); 400 kg (column No. 5); duration of pressure for a charge weighing 1 kg of TNT (column 6); 40 kg (column 7).

The pressure created by the air shock wave on the obstacle is always greater at the front of this wave if the angle of approach of the air shock wave to the obstacle is different from zero [12, 13].

When the air shock wave falls on a hard surface, the excess pressure in the reflected wave usually increases. In the plane wave approximation, the excess pressure in the reflected wave P_2 during direct reflection is determined by the formula [13]:

$$P_2 = P_1 + \frac{2kP_1(P_1 - P_0)}{(k-1)P_1 + (k+1)P_0}, \qquad (3)$$

where P_1 is the pressure at the front of the incident air shock wave; P_2 is the pressure at the front of the reflected air shock wave; P_0 is the initial pressure in the air; k is the adiabatic

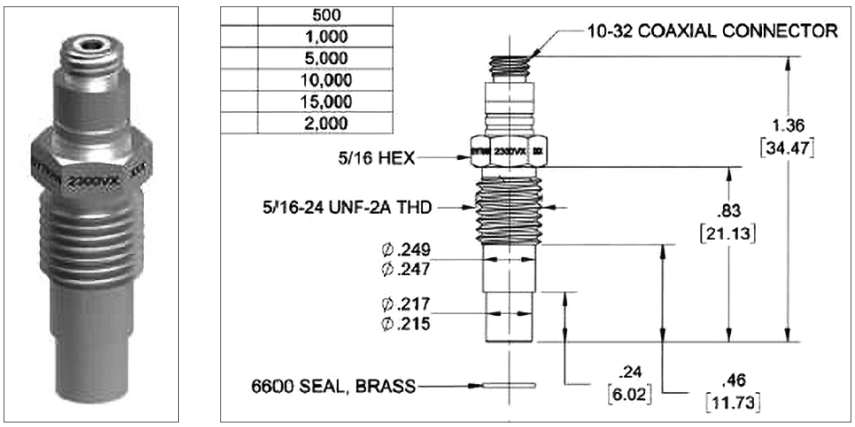

a) **b)**

F i g . 3. Dynamic pressure sensor type PS2300V5: photograph (a) and diagram (b)

Table 1. The magnitude of the excess pressure at the air shock wave front and the corresponding distances in m for charges of 1 kg, 40 kg and 400 kg

$p_1=\Delta p\cdot 10^{-5}$, Pa	R / R_0	R, m	R, m	R, m	τ_+, ms	τ_+, ms
1	2	3	4	5	6	7
10,22	20	1	3,4	7,36	1,17	
8,15	22	1,1	3,74	8,10	1,23	
6,34	24	1,2	4,08	8,83	1,28	
5,42	26	1,3	4,42	9,57	1,34	
4,58	28	1,4	4,76	10,30	1,39	
3,80	30	1,5	5,10	11,04	1,43	4,88
3,35	31,5	1,58	5,36	11,59	1,47	
2,94	33,4	1,67	5,65	12,25	1,51	

index of the air ($k = 1.4$ for an ideal gas). For a strong air shock wave ($P_1 >> P_0$), formula (3) gives $P_2 = 8P_1$. For $P_1 = 0.458$ MPa at $R \approx 28R_0$ (Table 1), $P_2 = 1.56$ MPa.

A distinction is made between regular and irregular (Makhov reflection). Makhov reflection with the formation of a Makhov wave in addition to the incident, reflected waves is realized when $\varphi > \varphi_{pr}$. The fronts of all waves converge to a single point (triple point), which moves at an angle to the reflection surface in a self-similar mode.

If the angle of incidence of the air shock wave on the obstacle is taken into account, the formula for the excess pressure in the reflected wave with regular reflection is a different approach [13]:

$$\frac{P_1}{P_0} = \frac{7}{6} M^2 \sin^2 \varphi_0 - \frac{1}{6} = \frac{7M_0^2 - 1}{6}; \quad (4)$$

$$;\frac{P_2}{P_1} = \frac{7}{6} M_1^2 \sin^2 \varphi_1 - \frac{1}{6}; \quad (5)$$

$$\varphi_2 = \varphi_1 - \theta\,. \quad (6)$$

where $M_0 = D_1/C_0$ – Mach number of the incident wave; $M = M_0/\sin\varphi_0$ – Mach number in the gas when passing through the seal jump; C_0 – velocity of sound in the gas at rest; φ_0 – angle of inclination of the seal jump relative to the reflection surface; M_1 – Mach number of the gas flow in the reflected wave; ϑ – angle of rotation of the gas flow through the incident air shock wave; φ_1, φ_2, – angles of inclination of the direct and reflected air shock wave.

Calculations using formulas (4–6) and others not given in this section for determining the parameters M_1, ϑ, $\varphi 1$, φ_2 are quite complex and can be used to solve specific problems of the interaction of the air shock wave with elements of structures and buildings. If the element of the structure or building is located at a large distance from the charge, then the curvature of the air shock wave front can be neglected and formulas (1–3) can be used to estimate the excess pressure and other parameters of the air shock wave action on the obstacle. When flowing around ($\varphi_0 = 90^\circ$) $M = M_0$ the pressure does not change.

When detonating a charge on a hard surface, when an air shock wave is formed in a half-space, it is necessary to substitute a doubled charge mass into the formulas. If the barrier is deformed and compressed, then part of the energy goes to its destruction and the formation of an air shock wave in it. Therefore, in the formulas for the air shock wave parameters, it is necessary to substitute the equivalent charge mass, which is equal to $2\eta C$, where the coefficient η takes into account the fraction of the explosion energy that is released into the air. For an absolutely hard barrier, $\eta = 1$. The value of the coefficient η for some barrier materials according to the data of work [13] is given in Table. 2.

Near the explosive charge, the law of attenuation of the air shock wave will be different from that shown by formula (1) [1]. At large distances from the charge, the propagation of the air shock wave passes into the acoustic stage. Some data for concentrated charges with spherical symmetry can be found in [12, 13]. For cylindrical charges, see [14].

Irregular reflection occurs only if the reflection angle exceeds approximately 40° and depends on the magnitude of the excess pressure in the incident air shock wave. From the point of view of the action of the air shock wave from an explosion in the air on structures, the greatest interest is the pressure ratio P_1 / P_2. This value changes with the change in the angle of incidence of the wave from $\varphi_0 = 0^\circ$ to $\varphi_0 = 90^\circ$ at a given intensity of the incident wave with the Mach number $M_0 = \text{const}$ (or $P_1 / P_0 = \text{const}$). As already noted, with direct reflection P_2 / P_1 is calculated by formula (3). With an increase in φ_0, the ratio P_2 / P_1 first decreases, and then with the approach of φ_0 to φ_{pr} it becomes equal, and for weak shock waves it is somewhat larger than with direct reflection. When switching to Mach reflection, P_2 / P_1 drops abruptly to a certain value and then smoothly decreases to $P_2/P_1 = 1$ at $\varphi_0 = 90^\circ$. A jump-like drop in P_2 / P_1 is observed with strong shock waves with $P_0 / P_1 \le 0.5$. For weak air shock waves, when transitioning to Mach reflection, there

Table 2. Values of the coefficient η for some barrier materials when detonating a charge on a hard surface

Type of obstacle	Steel plate	Reinforced concrete slab	Concrete, rocky soil	Dense loams, clays	Medium density soils	Water
η	1	0,95 – 1	0,85 – 0,9	0,7 – 0,8	0,6 – 0,65	0,55 – 0,6

is a slight smooth increase and then a sharp decrease in P_2 / P_1. In fact, formula (3) is universal for estimating the excess pressure «from above» on structures during air shock wave reflection.

RESULTS OF PHYSICAL SIMULATION

The results of physical simulation on an experimental stand using visual studies using a high-speed video camera and instrumental measurements of acoustic pressure on the surface of a ballistic foam concrete protective structure, as well as on the surface of a concrete structure protected by a layer of ballistic foam concrete, showed the following. As a result of video shooting, about 2 thousand video frames were obtained, which allowed us to determine in detail the features of the explosion formation from the process of its formation to degeneration. The features of the formation of an air shock wave, its time of existence and interaction with protective structures were determined.

Instrumental measurements of dynamic pressure from an air shock wave on the surfaces of the ballistic foam concrete test specimens No. 1 and No. 2 from their front and back sides are shown in Fig. 4a.

The measurement results show that the air shock wave pressure on the front surfaces of the ballistic foam concrete protective structure of models No. 1 and No. 2 is significantly higher (red and blue curves in Fig. 4) than on the back surface of the ballistic foam concrete or on the surface of the protected concrete wall model (green and purple curves). This confirms that the ballistic foam concrete protective layer of models No. 1 and No. 2 significantly reduces the air shock wave pressure generated by the detonation of a 1 kg TNT charge at a distance of 1.4–1.5 m from the ballistic foam concrete structure model, on the protected concrete wall by up to 10 times.

The results of measuring the dynamic pressure from the air shock wave generated by the detonation of a 1 kg TNT charge at a distance of 1.4–1.5 m from the model of the ballistic foam concrete structure, on the surfaces of the experimental ballistic foam concrete samples No. 3 and No. 4 from its front and back sides are shown in Fig. 4b.

As in the case of ballistic foam concrete protective structures models No. 1 and No. 2, significant decreases in the pressure of air shock waves on the ballistic foam concrete surface of models No. 3 and No. 4 on their front and rear surfaces were observed, see Fig. 5. At the same time, the pressure of the air shock wave was almost the same as in the conditions of explosion No. 1 (near ballistic foam concrete structure models No. 1 and No. 2), but the dynamic pressure on the rear part of the ballistic foam concrete structure or on the surface of the protected concrete wall became significantly lower. This corresponds to the results of comparing the indicators of dynamic pressure sensors on the front surface of the ballistic foam concrete structure (red and blue curves in Fig. 4b) and on the rear surface of the ballistic foam concrete protective structure (green and brown curves). The measurement results show that these ballistic foam concrete structure models dampen the air shock wave even more and the damping coefficient reaches several tens of times.

Comparing the results of calculations using formula (1) (Table 1) with experimental data, we can conclude that there is a satisfactory agreement in terms of the amplitude of the air shock wave and a much worse agreement in terms of the pulse duration (Table 1, Table 3). This difference can be explained by different atmospheric conditions: in our experiments the weather was rainy and the air humidity was (90–100) %. This increases the air density. In experiments [12] the humidity could be different. In addition, there were several reflection surfaces in the experimental conditions: sample No. 1 and No. 2, sample No. 3 and No. 4, soil, etc. (Fig. 1, Fig. 2). The reflection surface itself is not absolutely rigid, as for formula (3). It deforms and collapses during the reflection process. Additional pressure peaks that appeared after a certain period of time are associated with the reflection of air shock wave from the soil base and from the surrounding soil embankment (Fig. 4).

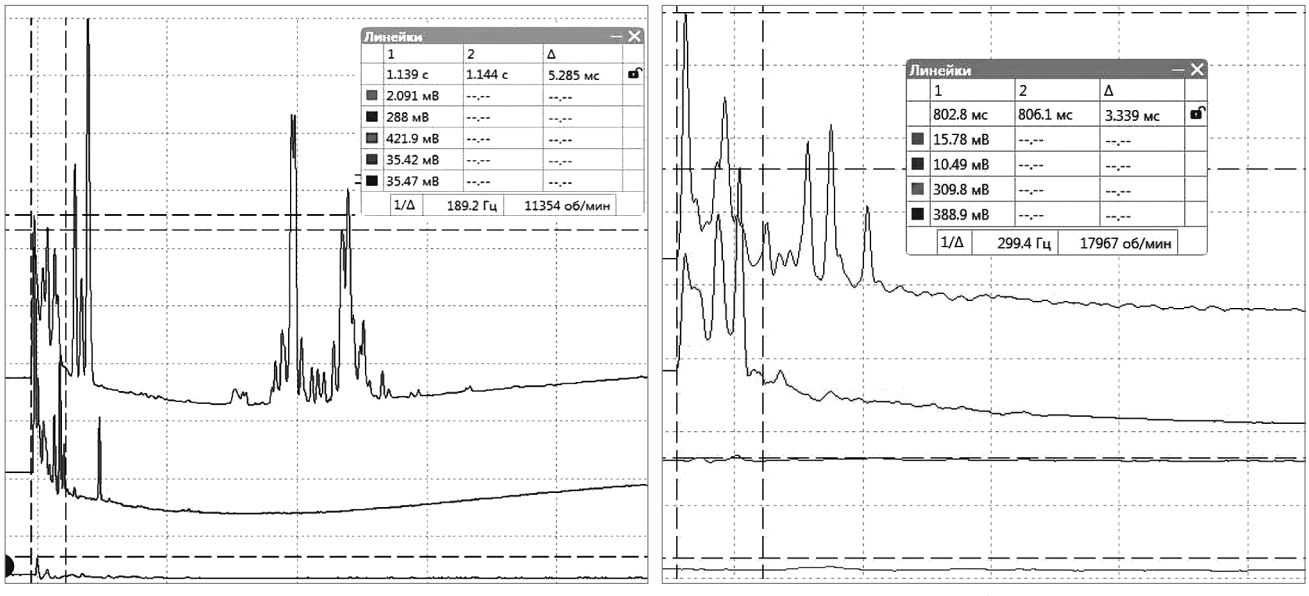

a) **b)**

F i g . 4. Shapes of pressure pulses on the surfaces of experimental samples of the ballistic foam concrete protective structures models No. 1 and No. 2 (a) and No. 3 and No. 4 (b)

Table 3. Parameters of dynamic pressure measurements during the fall and reflection of shock waves

Object / structure	Measuring instruments	Sensor readings, mV	Duration of pulsed pressure fluctuations, ms	Dynamic pressure*, at	Dynamic pressure drop (times)
Explosion No 1					
Experimental sample No. 1	External sensor No. 1	288	5,285	19,2	8,1
	Internal sensor No. 3	35,42	5,285	2,36	
Experimental sample No. 2	External sensor No. 2	421,9	5,285	28,12	11,9
	Internal sensor No. 4	35,47	5,285	2,37	
Explosion No 2					
Experimental sample No. 3	External sensor No. 5	388,9	3,339	25,93	24,7
	Internal sensor No. 7	15,78	3,339	1,05	
Experimental sample No. 4	External sensor No. 6	309,8	3,339	20,65	29,5
	Internal sensor No. 8	10,49	3,339	0,70	

Notes: * – dynamic pressure was calculated based on sensor calibration, 15 mV corresponds to 1 at.

After the blasting work, photo-fixation and measurement of the effects of air shock waves on the surface of the ballistic foam concrete protective structures samples were carried out. The results of the study showed that the shock waves from the explosions turned the relatively insignificant upper layer of the ballistic foam concrete slabs, which is the «sacrificial» layer, into compressed powder due to the destruction of interpore partitions. In the plane of the surface of the ballistic foam concrete slabs, the «sacrificial» layer was described by an imaginary circle, which is the projection of the explosion, with a diameter of about 1 m.

The thickness of the «sacrificial» layer decreased from the center of the circle to the periphery, and in the center of the circle was:

– (12–16) mm in test sample No. 1;
– (12–16) mm in test sample No. 2;
– (18–22) mm in test sample No. 3;
– (36–38) mm in test sample No. 4.

Fig. 5 presents photographs of the tested prototypes with the minimum and maximum thickness of the «sacrificial» layer.

Practical and scientific interests are the state of the entire ballistic foam concrete sample as a result of weakening the material throughout its depth by a direct wave of loading and unloading waves. For this purpose, methods of ultrasonic diagnostics of materials are used. A decrease in the velocity of ultrasound in the material indicates the appearance of new microcracks and cavities, which indicates a weakening of the strength properties of the material.

Researches of the attenuation of air shock wave in porous media were carried out quite widely, starting from the 60–70 s of the last century. These researches were carried out mainly with the aim of studying the effect of underground and surface nuclear explosions on underground structures and to study the dynamic properties of rocks and obtain shock adiabats [15, 16]. In particular, in [15] it is shown that the energy of the air shock waves E_{ASW} in a camouflage explosion in porous salt (NaCl) with a porosity of 2 %, 13.5 % and 20 % at relative distances from the charge $R / R_0 = (1–5)$ decreases in relation to the total energy E_0 of the explosion by approximately 0.7 to 0.1 and less for highly porous salt (20 %). The patterns

a) **b)**

Fig. 5. «Sacrificial» layer of the ballistic foam concrete slabs after explosions: test sample No. 1, with minimum layer thickness (a), test sample No. 4, with maximum layer thickness (b)

of attenuation of flat air shock wave in salt samples of different porosity as a result of impact with a flat aluminum impactor with an impact velocity of 1.7 km/s are also close to these patterns. The difference is only in the shape of the attenuation curves, which is explained by the geometry of the air shock wave front. According to these experimental data, at relatively large distances ≈(10–100)Δ (Δ is the thickness of the impactor, in our case, approximately the width of the air shock wave in the compression phase) the air shock wave attenuates 5–10 times depending on the porosity (2 %–20 %).

CONCLUSIONS

1. The results of the semi-real-life experiment showed that the parameters of the air shock wave from the explosion of a reference TNT charge weighing 1 kg (pressure in the reflected air wave) are in relatively satisfactory agreement with the data of calculations with empirical formulas of other authors.

2. It was determined that the dynamic pressure of the air shock wave on samples of ballistic foam concrete decreases on average by 8–30 times.

3. It was established that the dynamic shock pressure in the compression wave propagating through ballistic foam concrete, according to other authors, decreases by no more than 5–10 times.

4. It was shown that the thickness of the destruction zone of the ballistic foam concrete on the front side is not more than 20–40 mm. Spalling phenomena on the back side under the action of an air shock wave of low intensity (0.4-0.6) MPa were not observed.

5. It was established that the most effective in terms of protecting critical infrastructure facilities from the effects of air shock waves are the ballistic foam concrete protective structures of models No. 3 and No. 4, which are reinforced with fiber of composition «A» and «B» with an applied reinforcing layer of composite material, but at the same time, the deepest zones of destruction of ballistic foam concrete were observed on these models on the front side of the protective structure.

REFERENCES

1. Huang, C.-Y., Liu, F., Xin, K., Gao, Y.-H. & Duan, Y.-P. (2024). Research on shock wave driving technology of methane explosion. Scientific Reports. Vol. 14. P. 14897. https://doi.org/10.1038/s41598-024-65797-5.
2. Yang, Z., Cheng, J. & Zhang, B. (2024). Deflagration and detonation induced by shock wave focusing at different Mach numbers. Chinese J. Aeronautics. Vol. 37. No 2. Pp. 249—258. https://doi.org/10.1016/j.cja.2023.06.029.
3. Kozlov, P.V., Bykova, N.G., Gerasimov, G.Ya., Levashov, V.Yu., Kotov, M.A. & Zabelinsky, I.E. (2024). Radiation properties of air behind strong shock wave. Acta Astronautica. Vol. 214. Pp. 303—315. https://doi.org/10.1016/j.actaastro.2023.10.033.
4. Yang, Z. & Zhang, B. (2024). Investigation on the dynamics of shock wave generated by detonation reflection. Combustion and Flame. Vol. 270. P. 113791. https://doi.org/10.1016/j.combustflame.2024.113791.
5. Voskoboinick, V.A., Grinchenko, V.T. & Makarenkov, A.P. (2005). Pseudo-sound behind an obstacle on a cylinder in axial flow. Intern. J. Fluid Mech. Res. Vol. 32. № 4. Pp. 488—510. https://doi.org/10.1615/InterJFluidMechRes.v32.i4.60.
6. Voskoboinick, V., Kornev, N. & Turnow, J. (2013). Study of near wall coherent flow structures on dimpled surfaces using unsteady pressure measurements. Flow Turbulence Combust. Vol. 90. № 4. Pp. 709—722. https://doi.org/10.1007/s10494-012-9433-9.
7. Onyshchenko, A., Kovalchuk, V., Voskoboinick, V., Voskobiinyk, A., Aksonov, S., Trudenko, D. & Hrevtsov, S. (2024). Establishing patterns of change in the coefficients of reflection, transmission and dissipation of wave energy depending on parameters of a permeable vertical wall. Eastern-European J. Enterprise Technologies. No. 4/5(130). Pp. 46—56. https://doi.org/10.15587/1729-4061-2024.309969.
8. Bravo Celi, A., Falliano, D., Parmigiani, S., Suarez-Riera, D., Ferro, G.A. & Restuccia, L. (2025). Reuse of sheep wool fibers in the production of ultralightweight foamed concrete: effect of fiber treatment, length, and content on the mechanical properties. Fracture and Structural Integrity. Vol. 71. Pp. 317—329. https://doi.org/10.3221/IGF-ESIS.71.23.
9. Huang, H., Chen, F., Cao, K., Zhang, X. & Li, R. (2025). Damage evolution characteristics of steel-fiber-reinforced cellular concrete based on acoustic emission. Buildings. Vol. 15. P. 229. https://doi.org/10.3390/buildings15020229.
10. Irfanullah, Gul A., Khan, K., Khan, I.U., ElDin, H.M.S., Azab, M. & Shahzada, K. (2024). Improving the lateral load resistance capacity of cellular lightweight concrete (CLC) block masonry walls through ferrocement overlay. Applications in Engineering Science. Vol. 18. P. 100180. https://doi.org/10.1016/j.apples.2024.100180.
11. Lei, M., Liu, Z. & Wang, F. (2024). Review of lightweight cellular concrete: Towards low-carbon, high-performance and sustainable development. Construction and Building Materials. Vol. 429. P. 136324. https://doi.org/10.1016/j.conbuildmat.2024.136324.
12. Adushkin, V.V. & Korotkov, A.I. (1961). Parameters of the shock wave near the explosive charge during an explosion in air. PMTF. No. 5. Pp. 119—123.
13. Physics of explosion / Ed. Orlenko L.P. M.: Physmatlit. In 2 vol. 2004. Vol. 1. 832 p.
14. Tsikulin, M.A. (1960). Air shock wave during the explosion of a cylindrical charge of large length. PMTF. No. 3. Pp. 188—193.
15. Belinsky, I.V. & Khristoforov, B.D. (1976). On the dissipation of energy during an underground explosion. Explosive business. Coll. 76–33. M.: Subsoil. Pp. 178—184.
16. Mechanics. New in foreign science. Coll. of articles No. 26: Impact, explosion and destruction / Ed. Nikolaevsky V. N. M.: Mir. 1981. 239 p.

Войтенко Ю.І., Воскобійник В.А., Бойко В.В., Чепков І.Б., Остапчук Е.С., Немчин О.Ф., Євдощук Д.В.

ОЦІНКА ПАРАМЕТРІВ ПОВІТРЯНИХ УДАРНИХ ХВИЛЬ ТА ЗАХИСТ ВІД НИХ БАЛІСТИЧНИМ ПІНОБЕТОНОМ

Досліджено параметри повітряної ударної хвилі (ПУХ) при детонації стандартного заряду TNT (тротил) масою 1 кг при падінні її на перепони із балістичних пінобетонів чотирьох типів і обтіканні ПУХ цієї перепони. Товщина зразків пінобетону – 300 мм, щільність – 600 кг/м^3. Для розрахунків використано емпіричні формули Садовського М.А. Встановлено задовільний збіг експериментальних даних з параметрами, розрахованими за формулами Садовського М.А. В експериментах було показано, що амплітуда ПУХ за перепоною із пінобетону зменшується в середньому у 8–30 разів. Наближені оцінки за даними досліджень інших авторів (Белінский І.В., Христофоров Б.Д.) прогнозують зменшення хвилі стиснення, яка розповсюджується по пінобетону, не більше, ніж в 5–10 разів. В результаті експериментальних досліджень було установлено, що ударні хвилі від вибухів перетворили відносно незначний верхній шар пінобетонних плит, що є «жертовним» шаром, на спресований порошок, через руйнування міжпорових перегородок. У площині поверхні пінобетонних плит, «жертовний» шар описувався уявним колом, що є проекцією вибуху. Величина «жертовного» шару пінобетону, зруйнованого ПУХ з фронтальної сторони, не перевищує 20–40 мм. Відкольних явищ з тильної сторони на зразках пінобетону при падінні ПУХ амплітудою 0,4–0,6 МПа не спостерігалось. Виділено 2 типи балістичного пінобетону з найбільш ефективним гасінням хвилі стиснення в ньому. Установлено, що найбільш ефективними з точки зору захисту об'єктів критичної інфраструктури від дії повітряних ударних хвиль є пінобетонні моделі захисної споруди, які армовані фіброю складу «А» та «Б» з нанесеним посилюючим шаром композитного матеріалу. Визначено, що при цьому на цих моделях спостерігалися найглибші зони деструкції балістичного пінобетону з фронтальної сторони захисної споруди.

Ключові слова: *заряд, повітряна ударна хвиля, захисні споруди, пінобетон, критична інфраструктура, «жертовний» шар.*

Відомості про авторів:

Войтенко Юрій Іванович
доктор технічних наук, професор,
провідний науковий співробітник
Інститут гідромеханіки НАН України
м. Київ, Україна

Воскобійник Володимир Анатолійович
доктор технічних наук
старший науковий співробітник
завідувач відділу Інституту гідромеханіки НАН України
м. Київ, Україна
https://orcid.org/0000-0003-2161-6923

Бойко Віктор Вікторович
доктор технічних наук, професор
завідувач лабораторії
Інституту гідромеханіки НАН України
м. Київ, Україна

Чепков Ігор Борисович
член-кореспондент НАН України
доктор технічних наук, професор
начальник Центрального науково-дослідного інституту озброєння та військової техніки Збройних Сил України
м. Київ, Україна
https://orcid.org/0000-0002-4294-4152

Остапчук Едуард Станіславович
начальник відділу Центрального науково-дослідного інституту озброєння та військової техніки Збройних сил України
м. Київ, Україна
https://orcid.org/0000-0002-8095-0203

Немчин Олександр Федорович
доктор технічних наук, професор
провідний науковий співробітник
Інституту технічної теплофізики НАН України
м. Київ, Україна
https://orcid.org/0000-0001-9160-2768

Євдощук Дмитро Віталійович
головний інженер Інституту
технічної теплофізики НАН України
м. Київ, Україна

Information about the authors:

Voitenko Yuriy
Doctor of Technical Sciences, Professor
Leading Researcher of the Institute of Hydromechanics of the NAS of Ukraine
Kyiv, Ukraine

Voskoboinick Volodymyr
Doctor of Technical Sciences
Associate Professor
Head of Department of the Institute of Hydromechanics of the NAS of Ukraine
Kyiv, Ukraine
https://orcid.org/0000-0003-2161-6923

Boyko Viktor
Doctor of Technical Sciences, Professor
Head of the Laboratory of the Institute of Hydromechanics of the NAS of Ukraine
Kyiv, Ukraine

Chepkov Igor
Corresponding Member of the NAS of Ukraine
Doctor of Technical Sciences, Professor
Head of the Central Scientific Research Institute of Armament and Military Equipment of Armed Forces of Ukraine
Kyiv, Ukraine
https://orcid.org/0000-0002-4294-4152

Ostapchuk Eduard
Head of Department of the Central Scientific Research Institute of Armament and Military Equipment of Armed Forces of Ukraine
Kyiv, Ukraine
https://orcid.org/0000-0002-8095-0203

Nemchyn Oleksandr
Doctor of Technical Sciences, Professor
Leading Researcher of the Institute of Engineering Thermophysics
of the NAS of Ukraine
Kyiv, Ukraine
https://orcid.org/0000-0001-9160-2768

Yevdoshchuk Dmytro
Chief Engineer of the Institute of Engineering Thermophysics
of the NAS of Ukraine
Kyiv, Ukraine

The article was received by the editorial board on 04.03.2025.